Controlled Nucleation of GaN Nanowires Grown with Molecular Beam Epitaxy

By *Kris A. Bertness,* Aric W. Sanders, Devin M. Rourke, Todd E. Harvey, Alexana Roshko, John B. Schlager,* and *Norman A. Sanford*

The location of GaN nanowires is controlled with essentially perfect selectivity using patterned SiN_x prior to molecular beam epitaxy growth. Nanowire growth is uniform within mask openings and absent on the mask surface for over 95% of the usable area of a 76 mm diameter substrate. The diameters of the resulting nanowires are controlled by the size of the mask openings. Openings of approximately 500 nm or less produce single nanowires with symmetrically faceted tips.

1. Introduction

In this paper we show that GaN nanowires can be grown at predetermined locations through selective molecular beam epitaxy (MBE) in openings formed in SiN_x mask layers. This advance enables the growth of regular arrays of uniform GaN nanowire devices, which is essential for reliable manufacturing. The openings control both the position and the diameter of the nanostructures grown. When the openings are approximately 500 nm or less in diameter, the GaN forms a single nanowire with a distinct faceted end and excellent optical properties. Growth in larger openings displays a rough top surface which may indicate coalescence of multiple nanowires. By optimizing growth and processing conditions, essentially perfect selectivity, defined as the absence of GaN growth on the mask and uniform growth within mask openings, was achieved over at least 95% of the area of a 76-mm diameter substrate, excluding the outer 2 mm edge region of the wafer.

While selective epitaxy is commonly used in organometallic vapor phase epitaxy (OMVPE) growth processes, including those used for GaN nanowire growth,[1] these selective processes depend on the differences in reactivity between partially dissociated organometallic reagents and various surfaces. Both SiO_x and SiN_x make effective selective epitaxy masks over a broad range of growth parameters for trimethyl gallium and trimethyl indium.[2] Growth of GaN nanowires with OMVPE produces material with yellow luminescence[1] that is believed to be due to carbon incorporation.[3] As discussed further below, MBE growth produces nanowires of extremely high purity; however, the elemental Ga beam is highly reactive with most surfaces, and the only path to selective growth is through the use of high temperature where most of the Ga evaporates from one surface while incorporating, perhaps with low efficiency, to another. The only reported examples of truly selective GaN growth using MBE are for GaN nanowires grown in patterned nitrided titanium masks.[4] Although the titanium masks produced arrays of uniform, closely spaced wires (periodicity 800 nm or less) under the right growth conditions, the degree of selectivity was too low to prevent nucleation on large regions of mask material except in cases where very little material nucleated in the mask openings. The work in this paper thus illustrates the first combination of high material purity nanowire growth with high selectivity over wafer-scale areas.

Catalyst-free, MBE-grown GaN nanowires have been shown to be strain-free and of exceptionally high material quality.[5,6] The room-temperature photoluminescence lifetime of the nanowires can exceed 2.7 ns, with 900-nm diameter nanowires exhibiting longer lifetimes than smaller nanowires due to lower surface recombination rates.[7] These lifetimes generally exceed that of GaN material used in industrial applications such as high-brightness LEDs, even those manufactured with lateral epitaxial overgrowth (LEO)[8] or on nonpolar planes.[9] The exceptional properties of the nanowires are attributed in part to the lack of chemical impurities, leading to background carrier concentrations below 1×10^{16} cm^{-3} and low temperature optical emission spectra dominated by free and bound exciton emission with no observable visible emission. The nanowires grown with catalyst-free MBE are also free of structural defects such as threading dislocations, screw dislocations, and basal plane stacking faults. The growth axis is consistently along the *c* axis, or [0 0 0 1] direction, of the wurtzite crystal structure. The smooth *m*-plane sidewall surfaces (the {1 –1 0 0} family of six equivalent planes) are relatively nonreactive in air. This resistance to chemical attack probably contributes to their excellent mechanical quality factors Q, which regularly exceed 10 000.[10]

2. Results and Discussion

2.1. Selective Epitaxy Results

The primary driving force for the selective nucleation of the GaN nanowires is the difference in Ga sticking coefficient

[*] Dr. K. A. Bertness, Dr. A. W. Sanders, D. M. Rourke, T. E. Harvey, Dr. A. Roshko, Dr. J. B. Schlager, Dr. N. A. Sanford
NIST, Mail Stop 815.04
325 Broadway, Boulder, CO 80305 (USA)
E-mail: bertness@boulder.nist.gov

DOI: 10.1002/adfm.201000381

between the mask and the surface exposed in patterning of the mask. Typical results for selective epitaxy for SiN_x deposited on top of a thin layer of AlN are shown in **Figure 1**. The nanowires generally have well-formed hexagonal cross-sections, and there is no visible growth of GaN on the mask layer. The smallest wires have distinctly faceted tops with six facets that make angles of ~32° relative to the *c*–plane, which correspond to {1 –1 0 3} planes. As we have also observed for random nucleation,[5] the nanowires are aligned to the Si substrate with the GaN <1 –1 0 0> direction aligned with the Si <2–1–1> direction, and GaN <11–20> aligned with Si<1–10>.

The lateral dimension of the mask opening controls the development of the nanowire morphology, as shown in **Figure** 1 and **2**. For mask openings that are less than approximately 500 nm, the nanowires adopt the hexagonal cross-section morphology early in growth, when less than 250 nm tall. These nanowires exhibit the symmetrical end faceting described above (Figure 1b), and the diameter of the nanowire is controlled by the size of the opening. For larger mask openings, up to about 1000 nm, the wires continue to rapidly form hexagonal sidewalls and track the opening in diameter but the tops contain multiple random facets. For even larger openings (Figure 2c,d), the GaN growth develops *m*-plane sidewalls more slowly. These larger pillars also often display small voids at their base and occasional steps and faceting of sidewalls (Figure 1c), which implies that the pillars in these openings were produced by the coalescence of growth nucleating at multiple points within the opening. Even for the very largest openings, the tendency of the edges to conform to *m*-plane surfaces is evident in the smooth walls growing from openings already parallel to an *m*-plane while the edge perpendicular to the *m*-planes is faceted (top and bottom in Figure 2d).

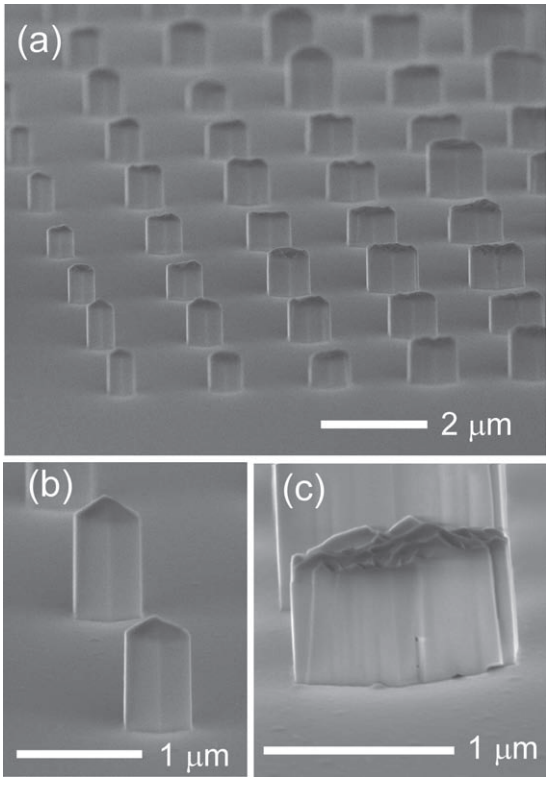

Figure 1. Arrays of selectively nucleated GaN nanowires with a FESEM view angle of 80° from the sample normal; a) array with openings from 500 to 1000 nm; b) close-up of nanowires growing in an opening of 500 nm; c) close-up of GaN in an opening with 1000 nm diameter from a different region on the same wafer.

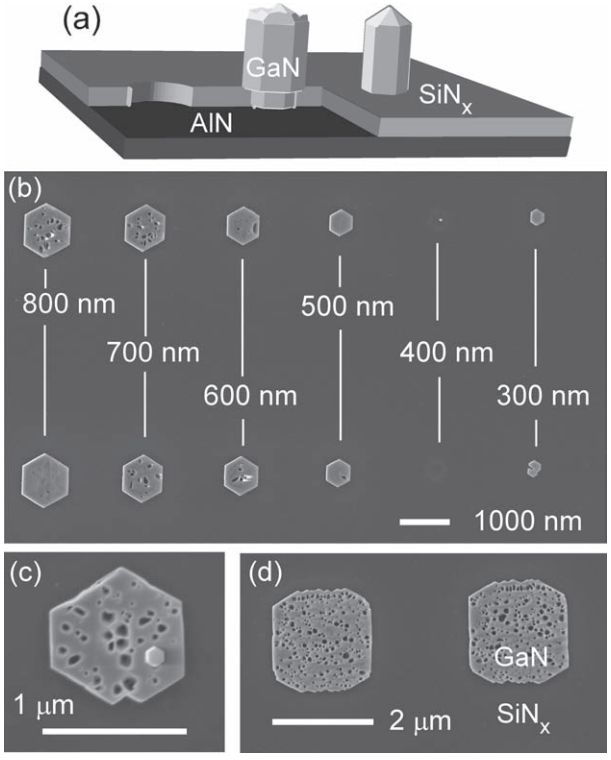

Figure 2. GaN selective area growth showing effect of mask opening dimensions on growth morphology. a) Schematic of the growth with perspective view with cut-away showing circular opening in mask down to the AlN layer and nanowire growth within the openings. b) Overhead-view images of nanowires grown in two rows with nominal opening diameter decreasing from left to right, as indicated; also shows effect of incomplete mask etching for 400 and 300 nm openings; c,d) openings were defined with photolithography and were initially rounded square openings. Note that the {1 –1 0 0} planes are still evident in d.

The material in the larger openings may have quite different properties than that of true nanowires, particularly with regard to being free of crystalline defects. In order to investigate the material quality, we performed room temperature photoluminescence (PL) experiments on the different array sizes (Figure S1 in Supporting Information). As expected, given that the growth conditions are nearly identical to those used for random nucleation, the nanowires in the array patterns are free of sub-band-gap luminescence, indicating that they are of high purity with few, if any, crystalline defects. The coalescence indicated by the FESEM images for mask openings in the 700 to 1400 nm range therefore does not automatically imply high defect densities. Coalesced GaN nanowires have been used as a template for high-quality GaN epilayer growth.[11] The PL intensity for nanowires larger than 750 nm

in diameter is slightly lower than that of smaller nanowires, indicating that the larger nanowires are slightly degraded, either by their larger effective surface area due to the deep corrugations in the top surface or by a low but finite dislocation density. The material in the mesas (openings >1 mm), however, has broad sub-gap luminescence centered on 2.0 eV indicating a high density of crystalline defects. This GaN material more closely resembles that of "matrix" material which grows in between nanowires under many, but not all, MBE nanowire growth conditions.[5] Matrix material usually exhibits mid-band-gap luminescence[12] and a high density of basal plane stacking faults. As shown in Figure 2c, true nanowire nucleation can occur within the pits of the faceted surface, but this type of nucleation is rare.

The high degree of uniformity of the selective area growth is illustrated in **Figure 3**. Several images were analyzed to determine the area and perimeter of nanowires within ensembles representing three different regions of the wafer and several mask opening diameters (see Supplemental Information). As can be seen in Figure 3, the fractional variation in the area is between 0.013 and 0.072, with better uniformity for the larger diameter openings where the variation is approximately equal to the estimated pixilation noise, shown with the dashed line. The image analysis program also estimates the circularity, defined as the ratio of the perimeter squared to 4π times the area. The circularity for a perfect hexagon is 1.103, which is achieved within measurement uncertainty for most of the patterns sampled. Because the growth processes should be more uniform for smaller feature sizes, the increase in area variations and shape imperfections for small openings is attributed to the variation in the development of the electron beam photoresist and subsequent etching.

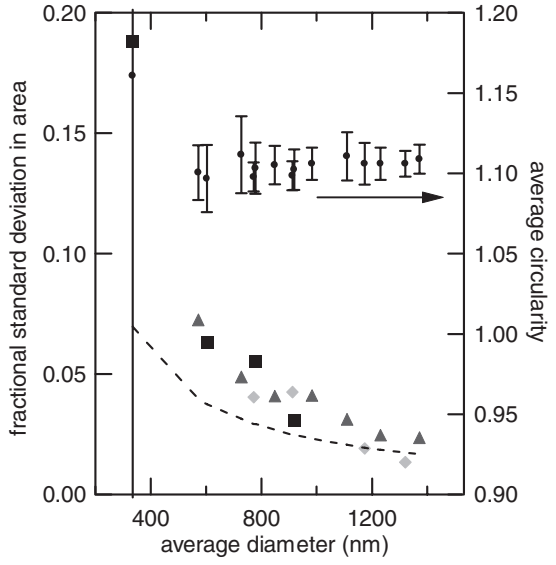

Figure 3. Variations in area for ensembles of nanowires as a function of average nanowire diameter. The three symbols represent three different regions of the wafer. The dashed line indicates the random variation expected from pixilation noise in the area determination. The circularity parameters, plotted against the right axis, are within experimental uncertainty identical to the value expected for a perfect hexagon, 1.103.

2.2. Selective Epitaxy Mechanism

The data in Figure 1 and 2 (and similar data not shown) demonstrate two attributes of the selective growth mechanism. First, the transition from symmetrically faceted tips to randomly faceted tips with increasing diameter suggests that the diffusion length of Ga atoms *on the nanowire surfaces* is about 200 nm to 300 nm under these growth conditions. Second, the vertical growth rate is independent of the nanowire diameter and the spacing between nanowires. This observation indicates that growth nucleation occurs at the same time (at the beginning of the growth run) for all the nanowires in fully etched mask openings. (Figure 2 also illustrates inhibition of growth in openings with diameter of 400 nm that failed to fully develop under the e-beam exposure used for this region, preventing the mask etch from exposing the underlying AlN.) The absence of systematic height variations with position in the center of arrays or at the edge indicates that the mask is neither a significant source or sink of reactants under conditions of high selectivity. This observation places an upper limit for diffusion of Ga *on the mask* of < 90 nm, or about one-fourth the minimum pattern spacing tested. The absence of a depletion zone around mask openings[13] under slightly altered conditions where GaN is just starting to nucleate on the mask indicates that the Ga evaporation from the mask, rather than diffusion to nanowire growth sites, is the dominant selectivity mechanism. Our result is thus distinct from the results of Kishino et al.,[4] where selectivity was significantly enhanced by close proximity of mask openings. This feature also distinguishes our results from the many selective epitaxy growth schemes in OMVPE, where vapor phase transport of unused reactants from mask regions to openings is often readily apparent in the accumulation of material at the mask edge.[14] We conclude that the residence time of Ga on the SiN_x mask is very short, that is, nearly all Ga landing on the mask desorbs.

Further information about the growth mechanism can be derived from the dependence of the vertical growth rate of various GaN features as a function of distance from the wafer center, illustrated in **Figure 4**. The features monitored are: 1) nanowires, labeled "NWs", 2) the edge of GaN growing in larger openings, labeled "mesas", examples of which are shown in **Figure 5**, and the 3) the matrix layer growing between nanowires. The Ga flux for all runs was such that if all impinging Ga atoms were incorporated, the thin film growth rate would be 60 nm h^{-1}. The Ga sticking coefficients represented by the data in Figure 4 are therefore on the order of 0.10 to 0.30. As would be expected for a growth temperature regime in which significant Ga evaporation occurs, the growth rate is higher for runs grown at approximately 10 °C lower growth temperature (runs A and C).

There is, however, a strong radial dependence to the growth rate, and, except for run A, the sign of this variation is opposite to the known decrease in substrate temperature as the distance from the wafer center increases. Most MBE growth sources have flux variations in which the flux decreases farther from the wafer center. The Ga flux distribution has been measured for this growth system, and the variation was found to be less than 10% out to 30 mm. Because the Ga flux variation is significantly less than the

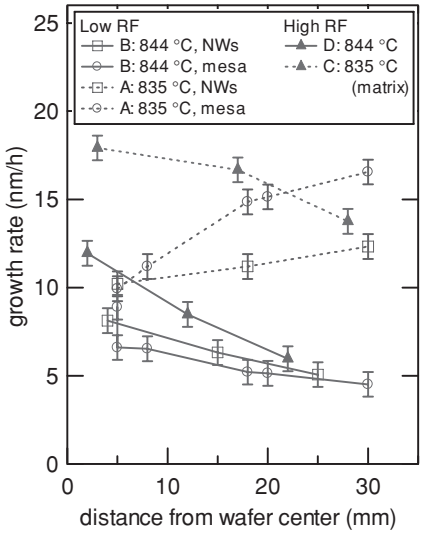

Figure 4. GaN growth rate variations from wafer center to outer edge during selective epitaxy under different substrate center temperatures and N_2 plasma RF power settings. The Ga flux used in these experiments would produce a film growth rate of 60 nm h^{-1} at unity sticking coefficient.

growth rate variation, we conclude that the variations in the N_2 plasma flux are responsible for the large decrease in growth rate approaching the wafer edge. The growths occur under conditions of large N_2 surplus, so it is unlikely that the N_2 flux is limiting the growth rate per se. The growth rate variations could instead be due to nonlinear increases in the Ga sticking coefficient in the presence of additional excited N species. Increased group-III sticking coefficient due to excess group-V availability is a well-known phenomenon in MBE crystal growth. This explanation is further supported by the experimental observation that the effect becomes less apparent at lower temperatures, when the Ga sticking coefficient is higher and therefore less sensitive to N flux. The effect also becomes more significant when higher radio frequency (RF) power is used with the plasma source (run C vs run A). The results suggest that increases in growth rate by lowering the growth temperature even further are probably feasible without sacrificing selectivity.

Another interesting feature is the growth parameter dependence for the morphology of GaN growing in the larger openings in the SiN_x mask, referred to as "mesas" in Figure 4 and illustrated in Figure 5. At the lower growth temperature used in run A, where the N_2 plasma effect on the Ga sticking coefficient is minimal, the growth rate in the center of large features is about 2.5× higher than at the edge (Figure 5c). This effect does not appear at higher growth temperature, where the growth rate is strongly dependent on N_2 flux as described above (Figure 5d). Field emission scanning electron microscopy (FESEM) micrographs of growth in the immediate vicinity of a mask edge (Figure 5a,b) show that the degree of lateral overgrowth of GaN onto the mask and the steepness of the edge sidewall are unaffected by the substrate temperature. This observation argues against the possibility that the sloped edge in Figure 5c is caused by Ga diffusing from the mesa onto the SiN_x and then desorbing. The rough surface produced in the mesa growth is also not conducive to efficient surface diffusion. Although we require more data to make a conclusive determination, one possible explanation is that the center of the openings is slightly cooler than the surrounding material due to greater radiative cooling from the rougher surface. We have observed that the temperature of substrates often drops slightly (about 10 °C) over the course of a run when the thermocouple temperature for the substrate heater remains constant. It is likely that the temperature gradient extends over a greater distance than the slope observed, and that the slope is instead terminated by saturation of Ga sticking coefficient as it approaches the maximum value of 1.0.

A key factor in the high degree of selectivity is thorough cleaning of the substrate. Atomic force microscopy (AFM) proved to be a useful tool in identifying thin layers of residual photoresist left on the wafer in the patterning process. As illustrated in the Supplemental Information, standard chemical cleaning with photoresist stripper left a thin residue near patterned features that had wrinkles roughly 15 nm thick. A 10-min reactive-ion etch (RIE) clean removed most of this material,

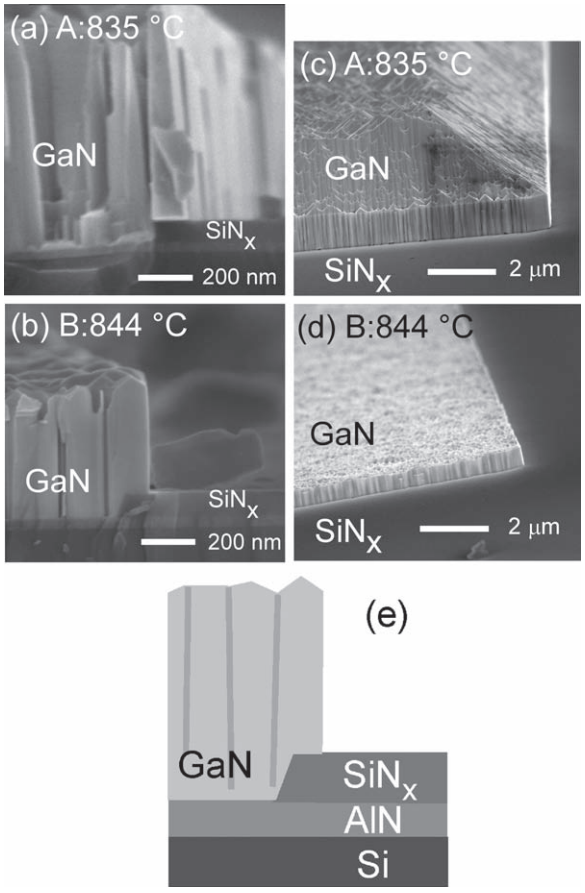

Figure 5. FESEM cross-sections (a,b) and 80° tilt views (c,d) of edges of large mask features, called "mesas" in the text. Note the slight overgrowth of GaN over SiN_x in both samples and the sharp sidewalls. Panels a and c are from run A, with growth temperature 835 °C, and b and d are from run B, with growth temperature 844 °C. e) Cartoon illustrating the layers present in a and b.

Table 1. Growth conditions. Growth temperatures are at wafer center.

Run	Growth temperature [°C]	RF power [W]	RIE cleaning [min]	Growth time [h]	SiN_x thickness [nm]
A	835	450 (24 h), 400	15	71	70–80
B	844	450 (6 h), 400	15	72	70–80
C	835	450	10	24	200–220
D	844	450	10	72	200–220

but thin lines remain between squares and at the edges of the squares. A 15-min RIE clean removed all traces of photoresist, with dramatic improvement in selectivity, also illustrated in the Supplemental Information.

3. Conclusions

GaN nanostructures were grown with essentially perfect selectivity on Si substrates using AlN buffer layers covered by patterned SiN_x mask layers. These nanostructures were single nanowires for openings approximately 500 nm in diameter or less. The diameter of the nanowire was determined by the size of the mask opening with slight expansion to achieve the preferred *m*–plane sidewalls. Material growing in large openings appeared to consist of coalesced nanostructures with rough, faceted tops. Medium openings, with diameters from 500 to 900 nm, yielded structures that appear to be single-crystal nanowires with multifaceted tops.

4. Experimental Section

Mask Fabrication and Patterning: AlN buffer layers were grown on Si(111) wafers by MBE to a thickness of 40 ± 8 nm. SiN_x was deposited on top of the AlN in a thermal furnace tube process with dichlorosilane and ammonia as reagents at a ratio of 5:1. The SiN_x films were grown at 835 °C and at a process pressure of 33 Pa (250 mTorr). The large features were patterned using conventional photolithography with repeating 1 cm^2 die that include arrays of 1 and 2 μm squares. The SiN_x was then etched down to the AlN buffer layer using CF_4/O_2 in a reactive ion etcher (RIE). The wafer was then coated with a tri-layer electron beam resist. Additional arrays of smaller circular openings were exposed and developed in the regions of the mask previously undisturbed in the photolithography step. These holes were transferred to the SiN_x with a second CF_4/O_2 etc. The resist was stripped from the surface using organic solvents. The wafer underwent a final clean using O_2 with the RIE system shortly before being loaded into the crystal growth system.

Molecular Beam Epitaxy: MBE growth was carried out in a commercial ultra high vacuum growth system with a Knudsen evaporator cell for Ga and RF plasma N_2 source for production of atomic N and excited molecular N_2 species. Growth conditions for the runs discussed in this paper are given in **Table 1**. The beam equivalent pressure (BEP) for Ga was 1.3×10^{-5} Pa (1.0×10^{-7} Torr). Calibration of the Ga flux with GaAs RHEED data taken close in time to the GaN growths indicated that a solid GaN film would grow at a rate of 60 nm h^{-1}. The plasma source N_2 was operated at 350 to 450 W RF forward power and a N_2 flow rate of 3 sccm, and the pressure in the plasma tube itself was approximately 120 Pa. Further details on GaN nanowire growth conditions and mechanism in this system have been previously published.[5,15]

Supporting Information

Supporting Information is available online from Wiley InterScience or from the author.

Acknowledgements

This work was partially supported by the DARPA Center on Nanoscale Science and Technology for Integrated Micro/Nano-Electromechanical Transducers (iMINT) funded by DARPA N/MEMS S&T Fundamentals Program (HR0011–06-1–0048) (Dr. D. L. Polla, Program Manager). Contribution of an agency of the U. S. government; not subject to copyright.

Received: February 27, 2010
Published online: July 13, 2010

[1] S. D. Hersee, X. Y. Sun, X. Wang, *Nano Lett.* **2006**, *6*, 1808.
[2] a) S. Keller, C. Schaake, N. A. Fichtenbaum, C. J. Neufeld, Y. Wu, K. McGroddy, A. David, S. P. DenBaars, C. Weisbuch, J. S. Speck, U. K. Mishra, *J. Appl. Phys.* **2006**, *100*, 054314; b) P. Deb, H. Kim, V. Rawat, M. Oliver, S. Kim, M. Marshall, E. Stach, T. Sands, *Nano Lett.* **2005**, *5*, 1847.
[3] A. Armstrong, Q. Li, K. H. A. Bogart, Y. Lin, G. T. Wang, A. A. Talin, *J. Appl. Phys.* **2009**, *106*, 053712.
[4] K. Kishino, H. Sekiguchia, A. Kikuchi, *J. Cryst. Growth* **2009**, *311*, 2063.
[5] K. A. Bertness, N. A. Sanford, J. M. Barker, J. B. Schlager, A. Roshko, A. V. Davydov, I. Levin, *J. Electron. Mat.* **2006**, *35*, 576.
[6] J. B. Schlager, N. A. Sanford, K. A. Bertness, J. M. Barker, A. Roshko, P. T. Blanchard, *Appl. Phys. Lett.* **2006**, *88*, 213106.
[7] J. B. Schlager, K. A. Bertness, P. T. Blanchard, L. H. Robins, A. Roshko, N. A. Sanford, *J. Appl. Phys.* **2008**, *103*, 124309.
[8] S. F. Chichibu, A. Uedono, T. Onuma, T. Sota, B. A. Haskell, S. P. DenBaars, J. S. Speck, S. Nakamura, *Appl. Phys. Lett.* **2005**, *86*, 124309.
[9] S. F. Chichibu, H. Yamaguchi, L. Zhao, M. Kubota, K. Okamoto, H. Ohta, *Appl. Phys. Lett.* **2008**, *92*, 091912.
[10] S. M. Tanner, J. M. Gray, C. T. Rogers, K. A. Bertness, N. A. Sanford, *Appl. Phys. Lett.* **2007**, *91*, 203117.
[11] T. Y. Tang, K. L. Averett, J. D. Albrecht, W. Y. Shiao, Y. S. Chen, C. C. Yang, C. W. Hsu, L. C. Chen, *Nanotechnology* **2007**, *18*, 445601
[12] L. H. Robins, K. A. Bertness, J. M. Barker, N. A. Sanford, J. B. Schlager, *J. Appl. Phys.* **2007**, *101*, 113506.
[13] S. C. Lee, S. R. J. Brueck, *Appl. Phys. Lett.* **2009**, *94*, 153110.
[14] a) Y. Honda, Y. Kuroiwa, M. Yamaguchi, N. Sawaki, *Appl. Phys. Lett.* **2002**, *80*, 222; b) X. Liu, D. E. Aspnes, *Appl. Phys. Lett.* **2009**, *94*, 253112.
[15] K. A. Bertness, A. Roshko, L. M. Mansfield, T. E. Harvey, N. A. Sanford, *J. Cryst. Growth* **2008**, *310*, 3154.